Research Square

Preprints are preliminary reports that have not undergone peer review.
They should not be considered conclusive, used to inform clinical practice,
or referenced by the media as validated information.

Innovative multi-phase corrective redispatch framework for restoration of voltage, frequency, and line limits under N-2 contingencies

Far Chen Jong

jongfc@icats.edu.my

i-CATS University College

Musse Mohamud Ahmed

Universal University of Science, Engineering & Technology

Research Article

Keywords: Decision support, N-2 contingencies, Optimal power flow, Corrective redispatch, Voltage, frequency, and line limit restoration

Posted Date: April 28th, 2026

DOI: https://doi.org/10.21203/rs.3.rs-9502431/v1

License: This work is licensed under a Creative Commons Attribution 4.0 International License.
Read Full License

Additional Declarations: No competing interests reported.

Innovative multi-phase corrective redispatch framework for restoration of voltage, frequency, and line limits under N-2 contingencies

Far Chen Jong [a,*], Musse Mohamud Ahmed [b,c]
[a] Faculty of Engineering and Technology, i-CATS University College, 93350 Kuching, Sarawak, Malaysia
[b] Universal University of Science, Engineering & Technology, Somalia
[c] Musse Innovative Sdn. Bhd., 93050 Kuching, Sarawak, Malaysia
* Corresponding author's email address: jongfc@icats.edu.my

ABSTRACT
Voltage, system frequency, and line loading are critical for power system security, especially under severe N-2 transmission line outages. Such contingencies can cause voltage violations, branch overloads, and frequency deviations, threatening system stability. Conventional contingency analyses are largely diagnostic and lack systematic corrective actions. This paper proposes a innovative multi-phase generator re-dispatch framework to mitigate operational violations following N-2 line tripping. A base-case AC power flow is established using MATPOWER, and N-2 contingencies are simulated by removing selected branches, generating during-contingency states with limit violations. An AC Optimal Power Flow (OPF) is then formulated to re-dispatch generators while enforcing voltage limits, generator capacities, and line thermal ratings. The fmincon interior-point solver was proposed and integrated into the framework to obtain the solution. System frequency deviation is analytically estimated from active power imbalances, enabling steady-state frequency assessment without dynamic simulation. Results on IEEE 14-bus and IEEE 118-bus test systems show all buses achieve full voltage compliance (100%) for all 8 cases, with the highest improvements of 78.57% for voltage, 16.67% for branch overload relief, and 0.166Hz for frequency, while maintaining execution times below 4.5 seconds, demonstrating a efficient and scalable decision-support tool for enhancing power system resilience.

KEYWORDS: Decision support; N-2 contingencies; Optimal power flow; Corrective redispatch; Voltage, frequency, and line limit restoration

1. Introduction

Voltage magnitude, system frequency, and transmission line loading must be maintained within prescribed limits to ensure secure power system operation, particularly under severe contingencies such as N-2 transmission line outages [1]. The simultaneous loss of two transmission elements can significantly alter power flow patterns, causing voltage deviations, thermal overloads, and degraded frequency performance [2]. If unmitigated, these violations may propagate and increase the risk of cascading failures or widespread instability. Voltage instability under contingency conditions is mainly linked to reactive power imbalances, insufficient local voltage support [3], and increased losses, potentially driving bus voltages outside the acceptable range of 0.95–1.05 p.u. [4]. Similarly, active power redistribution following outages may overload remaining corridors and violate thermal limits [5]. Although conventional contingency analysis tools effectively identify violations, they are largely diagnostic and provide limited corrective guidance [6], [7], [8].

These challenges are intensified by growing system complexity and high penetration of inverter-based renewable energy resources. Unlike synchronous generators, solar PV and wind sources provide limited inertia and reactive power support, complicating voltage and frequency control during disturbances [9]. Moreover, high network interconnectivity increases vulnerability to cascading overloads under N-2 events [10], [11]. Preventive methods such as SCOPF mainly enhance pre-contingency robustness but do not explicitly address post-contingency recovery. Consequently, corrective redispatch frameworks have emerged as practical solutions for restoring secure operation [12]. With advances in nonlinear programming, AC-OPF can re-dispatch generation while enforcing operational constraints, restoring voltage and frequency profiles and relieving line overloads without time-domain simulations [13].

Therefore, this paper proposes an innovative multi-phase corrective redispatch framework for restoring voltage, frequency, and line limits under N-2 contingencies. The approach integrates MATPOWER-based

contingency simulations with AC OPF re-dispatch solved using the fmincon interior-point algorithm. System performance is evaluated at three stages (pre-contingency, during contingency, and post-redispatch) to compare voltage profiles, line loading, and generator outputs. Steady-state frequency deviation is analytically estimated from active power imbalance to provide integrated frequency adequacy assessment.

The remainder of the paper is organized as follows. Section 1 reviews related work. Section 2 details the proposed methodology. Section 3 presents simulation results. Section 4 concludes the study and outlines future research directions.

1.1 Literature and Research Gap

Power system operation has long been based on the N-1 security criterion, requiring acceptable performance after any single outage [14]. However, major blackouts such as the 2003 North American event [15] and the 2006 European disturbance [16] showed that cascading failures often stem from multiple outages. Blackout statistics follow power-law behavior, underscoring the high impact of rare N-k events [17]. Thus, modern standards increasingly address instability and cascading risks under multiple contingencies. OPF minimizes generation cost subject to nonlinear power flow and operational constraints [18]. Security-Constrained OPF (SCOPF), including Preventive (PSCOPF), Corrective (CSCOPF), and hybrid (PCSCOPF) forms [19], explicitly models contingencies. PSCOPF is conservative and costly, while CSCOPF allows post-outage corrective actions, improving flexibility for severe N-2 events. Yet, SCOPF for higher-order contingencies faces scalability and modeling challenges in large systems [20]. Generator re-dispatch is a practical corrective measure for relieving congestion, restoring voltage, and maintaining security [12], and is easier to implement than topology reconfiguration [21]. Most re-dispatch studies focus on N-1 or separate voltage and congestion issues [22], while topology-based methods introduce mixed-integer complexity [23]. Frequency stability, affected by active power imbalance [24], is often overlooked in steady-state contingency studies [12], [25], [26].

Recent work spans metaheuristics [27], dynamic grid strength assessment [28], sensitivity-based methods [29], and evolutionary ranking [30], but many remain limited to N-1 [27], [26] focus on screening rather than mitigation [30], [31], [32], or rely on computationally intensive formulations [28], [33], [34], [25]. Fast N-2 screening methods [31], [13] often lack explicit corrective strategies, and several robust restoration approaches target distribution systems or long-term planning [35], [36], [25]. Frequency adequacy is frequently treated separately [28]. To address high-order contingencies (N-2, N-1-1, N-k) in renewable-dominated grids, advanced methods have emerged: PIGNN for accelerated screening [31], Quantum Contingency Analysis (QCA) [37], FSFRA for rapid reliability assessment [13], and ML/GPU-based prioritization [38]. Corrective strategies include Benders-based re-dispatch [34] and IVSI-integrated corrective SCOPF [12]. Modern indices such as NCPI [39], DGSI [28], and MSAI [40] enhance stability assessment, while resilience and security are strengthened through robust optimization [36], cyber-physical defense models [33], topology control via MISOCP [26], regional case studies [40], [41], RoCoF-based frequency metrics [42], adaptive inertia estimation [43], stochastic hybrid systems [44], harmonic-based ranking [45], thermostatic load support [46], sequential failure tools [47], reliability equivalents and Monte Carlo simulation [48], and spinning-reserve dispatch for dual threats [49]. Table 1 summarizes the reviewed literature, while Table 2 provides a comparative analysis between the proposed framework and existing state-of-the-art approaches.

Table 1: Summary of the reviewed literature

No	Area	Method	Merit	Demerit
[27]	Voltage Stability	Hybrid CF-PSO-Fuzzy AHP	Improves voltage profile and loadability (N-1).	High nonlinearity; costly if misallocated.
[28]	IBR Grids	DGSI (time-domain)	Captures transient/IBR tripping effects.	Computationally intensive.
[29]	AC-DC Networks	Z-bus distribution factors	Linear, non-iterative, generic.	~3% current redistribution error.
[30]	Transmission Security	Evolutionary algorithms	Effective critical line ranking.	Exploration–exploitation imbalance.
[33]	Infrastructure Resilience	NFE C&CG	Near-global defense strategy in minutes.	Approximate lower-level modeling.
[34]	Relay Security	Benders Decomposition	Avoids unintended relay tripping.	Runtime grows with contingencies.

[35]	Distribution/DER	GWO	↑ line capacity, ↓ losses (~23%).	Limited to radial systems.
[31]	N-2 Screening	Physics-informed GNN	37× faster than simulations.	Internal features lack exact physics.
[13]	Reliability	FSFRA (DCOPF/ACOPF)	2000× faster N-2 analysis.	Storage pre-dispatch ≈80% error source.
[36]	Distribution	Robust microgrid restoration	Enhances resilience in extreme events.	Conservative solutions.
[25]	Bulk Restoration	Bi-level robust optimization	Reduces outage losses robustly.	High computational burden.
[32]	Regional Planning	FDPF + sensitivity	Very fast contingency screening.	Inefficient for cascading outages.
[39]	Voltage Stability	NCPI	Identifies weak buses/loadability.	Steady-state only; topology sensitive.
[26]	Topology Control	MISOCP + NLP	Ensures AC feasibility & N-1 compliance.	Requires pre-screening for tractability.

Table 2: Comparison of the proposed solution against state-of-the-art approaches

No	N-2 Contingency?	System Limit Evaluation				Corrective Action				Benchmark with small system?	Benchmark with large system?
		V	P, Q	MVA	f	V	P, Q	MVA	f		
[34]	×	✓	✓	✓	✓	✓	✓	×	✓	✓	✓
[12]	✓	✓	✓	✓	×	✓	✓	✓	×	×	✓
[25]	✓	✓	✓	✓	×	✓	×	✓	×	×	✓
[26]	×	✓	✓	✓	×	✓	×	✓	×	✓	✓
[50]	×	✓	✓	×	×	✓	✓	×	×	✓	✓
[13]	✓	×	✓	✓	×	×	×	×	×	✓	✓
[33]	✓	×	×	✓	×	×	×	✓	×	✓	✓
[27]	×	✓	×	✓	×	✓	×	×	×	✓	×
[30]	×	✓	×	✓	×	×	×	×	×	✓	×
[28]	✓	✓	×	×	×	×	×	×	×	✓	×
[38]	×	✓	×	✓	×	×	×	×	×	✓	×
[51]	✓	✓	✓	×	✓	✓	×	×	×	✓	×
Proposed Solution	✓	✓	✓	✓	✓	✓	✓	✓	✓	✓	✓

To address the identified research gaps, this paper presents an innovative and practical multi-phase corrective redispatch framework that explicitly targets severe N-2 transmission contingencies and bridges conventional steady-state contingency analysis with actionable operational decision support. The originality of this work lies in its unified approach that systematically evaluates system performance before, during, and after contingencies, while actively restoring voltage, thermal, and frequency security through AC-feasible generator redispatch via OPF. An analytical steady-state frequency deviation assessment based on active power imbalance is incorporated within the same workflow, enabling coordinated mitigation of voltage violations, line overloads, and frequency deviations. The novelty of the framework lies in its integrated, computationally efficient design, implemented in MATPOWER with an interior-point solver, which avoids mixed-integer and dynamic simulation complexity and allows near real-time corrective decision support. By structuring the analysis into pre-contingency, during-contingency, and post-redispatch phases, the framework provides a practical and actionable tool that moves beyond preventive or purely diagnostic approaches under severe N-2 outage scenarios.

2. Methodology

This research presents a multiphase framework to evaluate N-2 branch contingencies and corrective generator redispatch on voltage, line loading, and frequency. Using MATLAB and MATPOWER 8.0 with IEEE benchmarks, it sequentially executes base-case power flow, contingency simulation, and AC OPF-based corrective redispatch.

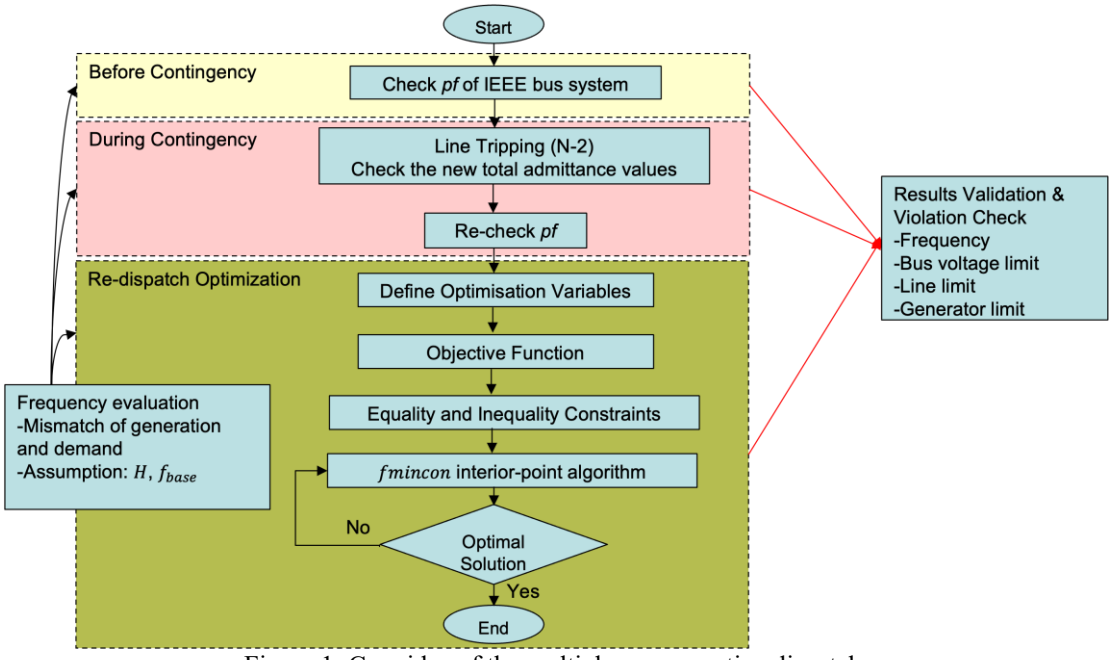


Figure 1: Core idea of the multiphases corrective dispatch.

2.1 Base Case Power Flow and Frequency Estimation

The first stage establishes the system's normal operating condition by solving the steady-state AC power flow using the Newton-Raphson method for its quadratic convergence and robustness. The power flow equations are as (1).

$$f(x) = \begin{bmatrix} P_i^{calc} - P_i^{spec} \\ Q_i^{calc} - Q_i^{spec} \end{bmatrix} = 0 \quad (1)$$

Where the state vector $x = [\theta, V]^T$ contains bus voltage angles θ_i and magnitudes V_i. Iterative Jacobian updates match calculated active and reactive power injections to specified values. Base-case variables, including generator outputs (P_{Gi}, Q_{Gi}), bus voltages, phase angles, and branch flows are obtained, with branch loading computed from apparent power magnitudes. Steady-state frequency deviation is estimated via the aggregated imbalance model as (2) to (4).

$$\Delta f = -\frac{\Delta P}{2Hf_o} \quad (2)$$

$$\Delta P = P_{gen} - P_{load} \quad (3)$$

$$f = f_o + \Delta f \quad (4)$$

Where f_o = 50 Hz, H is system inertia, P_{gen} is total generation, and P_{load} is total demand. This provides a steady-state frequency approximation suitable for contingency screening without dynamic simulation.

2.2 N-2 Contingency Simulation

In the second stage, system resilience under severe topological disturbances is assessed by simulating N-2 transmission contingencies. An N-2 event is modeled by the simultaneous removal of two transmission branches, represented as (5).

$$B' = B \setminus \{l_1, l_2\} \quad (5)$$

Where B and B' are the original and modified branch sets, and l_1, l_2 are the outaged lines. AC power flow is solved on the modified network to obtain bus voltages, phase angles, generator outputs, and branch flows.

Voltage violations and thermal overloads are identified against operational limits, and frequency deviation is recalculated using the aggregated imbalance to evaluate system frequency adequacy.

2.3 Post-Contingency Re-dispatch via AC Optimal Power Flow

To restore system security after N-2 contingencies, a corrective AC-OPF is formulated and solved using an interior-point method. The objective is to minimize generator re-dispatch as (6).

$$\min_{P_G, P_Q} \sum_{i \in G} (P_{Gi} - P_{Gi}^{o})^2 \tag{6}$$

Where P_{Gi}^{o} is the base-case generator output and P_{Gi} is post-contingency active power. The AC power flow constraints, generator limits, bus voltage magnitude constraints and transmission limits are as (7) to (14).

$$P_i(V, \theta) = \sum_j V_i V_j |Y_{ij}| \cos(\theta_i - \theta_j - \delta_{ij}) \tag{7}$$

$$Q_i(V, \theta) = \sum_j V_i V_j |Y_{ij}| \sin(\theta_i - \theta_j - \delta_{ij}) \tag{8}$$

$$P_i(V, \theta) - P_{i,spec} = 0 \tag{9}$$

$$Q_i(V, \theta) - Q_{i,spec} = 0 \tag{10}$$

$$P_{min,i} \leq P_{Gi} \leq P_{max,i} \tag{11}$$

$$Q_{min,i} \leq Q_{Gi} \leq Q_{max,i} \tag{12}$$

$$V_{min,i} \leq V_i \leq V_{max,i} \tag{13}$$

$$S_{ij} \leq k\, S_{max,ij} \tag{14}$$

Where k represents a permissible overload factor if emergency ratings are considered. To solve this constrained optimization problem, the Lagrangian function is constructed as (15).

$$\mathcal{L}(x, \lambda, \mu) = J(x) + \sum_{i=1}^{n} \lambda_i g_{eq,i}(x) + \sum_{j=1}^{m} \mu_j g_{ineq,j}(x) \tag{15}$$

Where $g_{eq,i}(x) = 0$ are the equality constraints (power balance equations), $\mu_j g_{ineq,j}(x) \leq 0$ are the inequality constraints (generator, voltage, and branch limits), λ_i are Lagrange multipliers associated with equality constraints, and $\mu_j \geq 0$ are Lagrange multipliers associated with inequality constraints. The Lagrangian transforms the constrained optimization into a single function whose gradient must vanish at the optimum, allowing iterative solution via interior-point or Newton-based methods. The interior-point method solves the AC-OPF by iteratively updating the decision variables and multipliers. In the begining, decision variables, x as (16) are initialized using post-contingency values.

$$x = [P_{Gi}, Q_{Gi}, V_i, \theta_i] \tag{16}$$

Lagrange multipliers λ_i and μ_j are initialized to small positive values. Then, computation of the Lagrangian gradient is peformed using (17),

$$\nabla_x \mathcal{L}(x, \lambda, \mu) = \nabla_x J(x) + \sum_i \lambda_i \nabla_x g_{eq,i}(x) + \sum_j \mu_j \nabla_x g_{ineq,j}(x) \tag{17}$$

Where ∇_x is the gradient operator with respect to the vector of decision variables x. Then, the step update is as (18),

$$x_{new} = x - \alpha H_{\mathcal{L}}^{-1} \nabla_x \mathcal{L}(x, \lambda, \mu) \tag{18}$$

Where $H_{\mathcal{L}} = \nabla_x^2 \mathcal{L}(x, \lambda, \mu)$ s the Hessian matrix of the Lagrangian, and α is a step-size parameter ensuring convergence and feasibility. The equality multipliers, λ_i are updated to enforce power balance and inequality multipliers, μ_j are updated using barrier or penalty methods to maintain feasibility ($\mu_j \geq 0$). The

convergence criteria (19)-(21) are deployed to ensure the iteration continues until all constraints are satisfied and the generator deviation objective is minimized.

$$|\nabla_x \mathcal{L}| < \in \quad (19)$$
$$g_{eq,i}(x) < \in \quad (20)$$
$$g_{ineq,j}(x) \leq 0 \quad (21)$$

Where $\in$ denotes the norm of the gradient is less than the small tolerance, indicating stationarity (the optimum has been reached with respect to x). After convergence, post-OPF results are recomputed using $\mathrm{Comp_r}$ as in (22). The post-OPF results ensure all bus voltages, branch flows, and system frequency are restored within operational limits, completing the corrective dispatch.

$$\mathrm{Comp_r} = \begin{cases} S_{ij_opt} = \sqrt{(P_{ij})^2 + (Q_{ij})^2} \\ V_{i_opf}, \theta_{i_opf} \\ P_{Gi_opf}, Q_{Gi_opf} \\ f_{opt} = f\left(P_{gen,opf}, P_{load,opf}, H, f_0\right) \end{cases} \quad (22)$$

2.4 Pseudocode Overview and Operational Limits

A pseudocode workflow of the corrective AC-OPF process as depicted in Figure 2 is used to illustrate the overall procedure clearly. The frequency, voltage and thermal limits should be controlled within the tolerable ranges to prevent grid system collapse; therefore, their operational limits and base value are shown in Table 3.

BEGIN
%% INITIALIZE SYSTEM
Load IEEE bus system case (mpc)
Set base frequency: f_0
Set system inertia: H
Define bus voltage limits: V_{min}, V_{max}
Define branch thermal limits: $S_{max,ij}$
Define generator limits: $P_{min,i}$, $P_{max,i}$, $Q_{min,i}$, $Q_{man,i}$
%% FREQUENCY ESTIMATION FUNCTION
FUNCTION f (P_{gen}, P_{load}, H, f_0)
  ΔP = SUM(P_{gen}) - SUM(P_{load})
  $\Delta f = -\Delta P / (2Hf_0)$
  $f = f_0 + \Delta f$
  RETURN f
END FUNCTION
%% STEP 1: BASE CASE POWER FLOW
Solve AC power flow using Newton-Raphson:
  FOR each bus i in 1…n
    Solve:
    $P_{i,cal} = \sum_j |V_i||V_j|(G_{ij}\cos\theta_{ij} + B_{ij}\sin\theta_{ij})$
    $Q_{i,cal} = \sum_j |V_i||V_j|(G_{ij}\sin\theta_{ij} + B_{ij}\cos\theta_{ij})$
    Subject to:
      $P_{i,cal} - P_{i,spec} = 0$
      $Q_{i,cal} - Q_{i,spec} = 0$
  END FOR
Compute generator dispatch: P_{Gi}, Q_{Gi}
Compute branch flows: $S_{ij} = \sqrt{(P_{ij})^2 + (Q_{ij})^2}$
Compute system frequency: $f_{base} =$ f ($P_{gen,base}$, $P_{load,base}$, H, f_0)
%% STEP 2: N-2 CONTINGENCY SIMULATION
Select contingency branches: l_1, l_2
Remove contingency branches from network
Solve AC power flow on modified network:
  FOR each bus i in 1…n
%% STEP 3: AC OPTIMAL POWER FLOW (POST-CONTINGENCY)
x = [P_{Gi}, Q_{Gi}, V_i , θ_i] for all generators and buses
Minimize J(x) = $\min_{P_G,P_Q} \sum_{i\in G}(P_{Gi} - P_{Gi}^o)^2$
FOR each bus i in $1\ldots n$
  $P_{i,cal(x)} = \sum_j |V_i||V_j|(G_{ij}\cos\theta_{ij} + B_{ij}\sin\theta_{ij})$
  $Q_{i,cal(x)} = \sum_j |V_i||V_j|(G_{ij}\cos\theta_{ij} + B_{ij}\sin\theta_{ij})$
  ENFORCE:
    $P_{i,cal} - P_{i,spec} = 0$
    $Q_{i,cal} - Q_{i,spec} = 0$
END FOR
FOR each generator i
  $P_{Gi,min} \leq P_{Gi} \leq P_{Gi,max}$
  $Q_{Gi,min} \leq Q_{Gi} \leq Q_{Gi,max}$
END FOR
FOR each bus i
  $V_{min} \leq |V_i| \leq V_{max}$
END FOR
FOR each branch $i-j$
  $S_{ij(x)} = \sqrt{(P_{ij})^2 + (Q_{ij})^2} \leq k\, S_{max,ij}$
END FOR
Initialize Lagrange multipliers λ_i for equality, μ_i for inequality
WHILE not converged:
  Compute Lagrangian:
  $\mathcal{L}(x,\lambda,\mu) = J(x) + \lambda^T g_{eq}(x) + \mu^T g_{ineq}(x)$
  Compute gradient $\nabla_x \mathcal{L}(x,\lambda,\mu) = \nabla_x J(x) + \sum_i \lambda_i \nabla_x g_{eq,i}(x) + \sum_j \mu_j \nabla_x g_{ineq,j}(x)$
  Update x using Newton step: $x_{new} = x - \alpha H_{\mathcal{L}}^{-1} \nabla_x \mathcal{L}(x,\lambda,\mu)$
  Enforce constraints and bounds
END WHILE
Compute branch flows: $S_{ij_opt} = \sqrt{(P_{ij})^2 + (Q_{ij})^2}$
Compute bus voltages: $V_{i_opf}, \theta_{i_opf}$

Solve: $P_{i,cal_cont} = \sum_j \lvert V_i \rvert \lvert V_j \rvert (G_{ij} \cos\theta_{ij} + B_{ij} \sin\theta_{ij})$ $Q_{i,cal_cont} = \sum_j \lvert V_i \rvert \lvert V_j \rvert (G_{ij} \cos\theta_{ij} + B_{ij} \sin\theta_{ij})$ END FOR Compute generator dispatch: P_{Gi_cont}, Q_{Gi_cont} Compute branch flows: $S_{ij_cont} = \sqrt{(P_{ij})^2 + (Q_{ij})^2}$ Compute system frequency: $f_{cont} =$ $f(P_{gen,cont}, P_{load,cont}, H, f_0)$	Compute generator outputs: P_{Gi_opf}, Q_{Gi_opf} Compute system frequency: $f_{opt} =$ $f(P_{gen,opf}, P_{load,opf}, H, f_0)$ **%% STEP 4: OUTPUT RESULTS** FOR buses i: Display V_i, θ_i FOR generators i: Display P_{Gi}, Q_{Gi}, $P_{Gi,min}$, $P_{Gi,max}$, $Q_{Gi,min}$, $Q_{Gi,max}$ FOR branches i, j: Display S_{ij}, $S_{max,ij}$ Display system frequency: f_{base}, f_{cont}, f_{opt} END

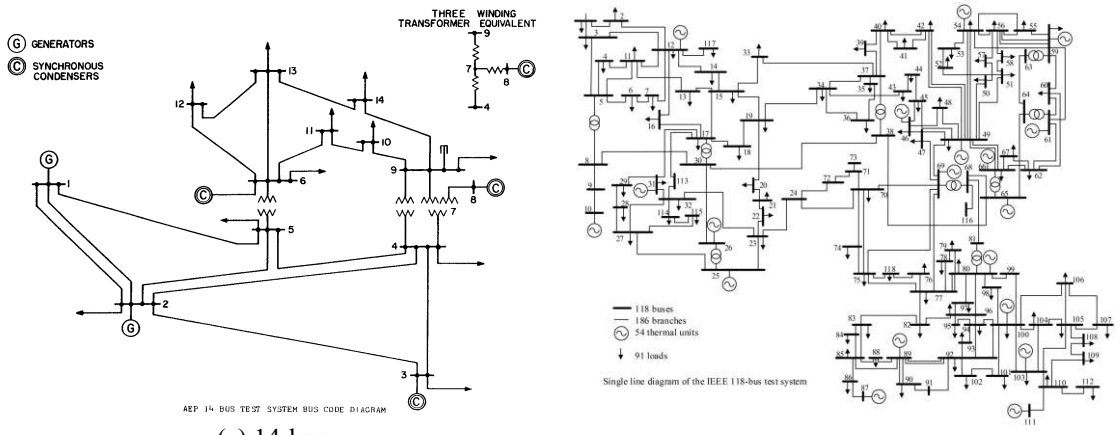
Figure 2: Pseudocode workflow of the proposed methodology.

Table 3: Operational limits of parameters

No	Parameter	Value
1	$P_{Gi,max}, P_{Gi,min}$, $Q_{Gi,max}, Q_{Gi,min}$	Defined according to generator capabilities (per IEEE bus model)
2	V_{min}, V_{max}	0.95 – 1.05 p. u., 0.97 – 1.03 p. u. (stringent case)
	f_{min}, f_{max}	49.5 – 50.5 Hz
3	Base MVA	100 MVA
4	Base Frequency	50 Hz
5	Inertia Constant	Assume 5s

3. Results and Discussion

The proposed corrective generator OPF methodology was evaluated for scalability and computational efficiency on two IEEE benchmark systems. The IEEE 14-bus system is a small-scale network with 14 buses, 5 generators, and 11 loads representing a simplified American Electric Power system (Feb 1962), while the IEEE 118-bus system is a large-scale network with 118 buses, 19 generators, 35 synchronous condensers, 177 lines, 9 transformers, and 91 loads, approximating the U.S. Midwest network (Dec 1962) with assumed line MVA limits for contingency analysis. The framework tested voltage, thermal, and frequency constraint handling under increasing network complexity. Computational efficiency was measured using MATLAB's $\text{tic} - \text{toc}$ for the before-contingency, during-contingency, and post-redispatch phases. Results show the method efficiently computes generator re-dispatch while maintaining operational limits and minimal deviation from base schedules. Figures 3(a) and 3(b) illustrate the IEEE 14-bus and 118-bus system topologies, showing generator and load locations relevant for N-2 contingency analysis.



(a) 14-bus (b) 118-bus

Figure 3: IEEE bus test systems diagram.

3.1 Results for IEEE-14 Bus Test System (Case: 1-4)

This section evaluates the performance of the proposed generator redispatch under multiple N-2 line outages, based on voltage profiles, generator outputs, branch loading, and system frequency (Figures 4–11). Figure 4 illustrates Case 1: outage of branches 1-5 and 2-5, with voltages constrained between 0.95–1.05 p.u. During the contingency (Figure 4a), mid-network buses show noticeable voltage dips, while some upstream buses exhibit mild overvoltage. Post-redispatch, voltages are restored uniformly within limits, indicating effective spatial redistribution of reactive power. Generator outputs (Figure 4b) initially show unequal burden, with one generator increasing sharply while others reduce output; redispatch balances contributions, enhancing operational margins. Branch flows (Figure 4c) increase along rerouted paths during the contingency but are reduced after optimization, showing that redispatch alone can relieve structural congestion. A small frequency dip occurs during the outage (Figure 4d), which is corrected after redispatch, promptly restore active power balance and support near-real-time corrective action. Case 2 (Figure 5) considers the same branch outages as Case 1 but with tighter voltage limits (0.97-1.03 p. u.). During the contingency, voltage deviations appear more critical relative to the stricter bounds, and post-redispatch voltages cluster tightly, showing recovery is constraint-driven. The system operates closer to optimal voltage stiffness, enhancing insulation margins and equipment lifespan. Generator adjustments are smaller but more numerous, reflecting a shift from corrective actions to distributed fine-tuning, which increases robustness but requires coordinated response. Peak branch flows are lower than in Case 1, as tighter voltage control reduces reactive circulation and indirectly mitigates thermal stress. Frequency deviations are also slightly smaller, indicating that enhanced voltage discipline improves overall system stiffness and supports frequency stability.

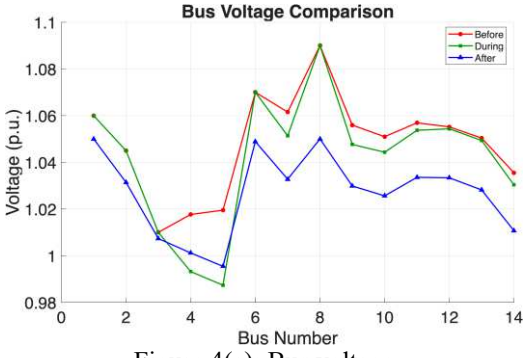


Figure 4(a): Bus voltage

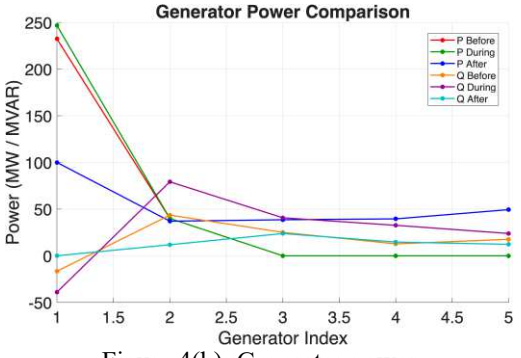


Figure 4(b): Generator power

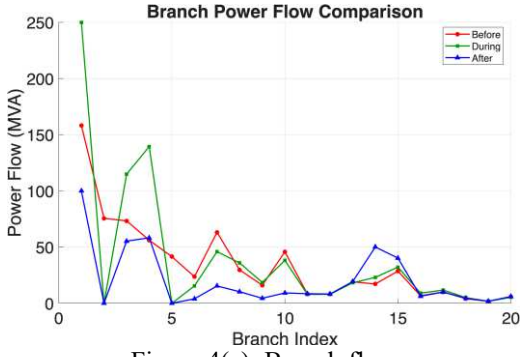


Figure 4(c): Branch flow

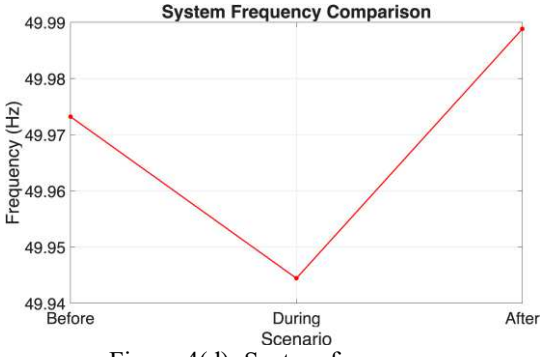


Figure 4(d): System frequency

Figure 4: Case 1: Outage of branches 1-5 and 2-5 (Voltage range: 0.95-1.05 p. u.).

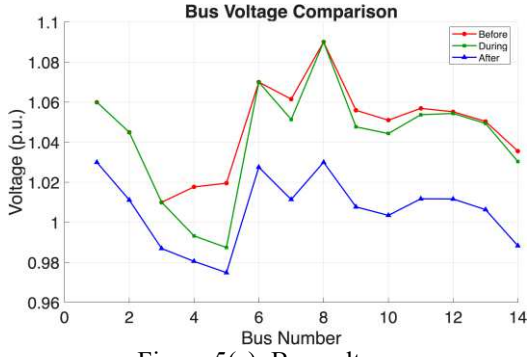


Figure 5(a): Bus voltage

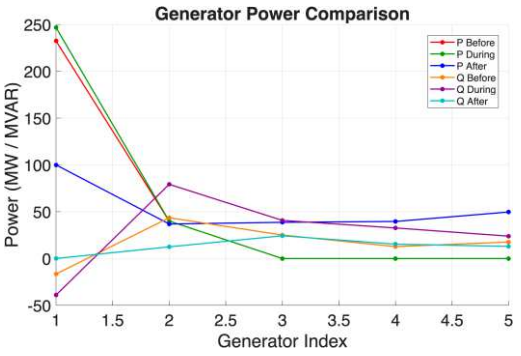


Figure 5(b): Generator power

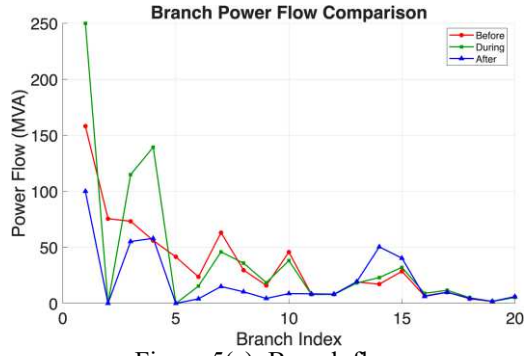


Figure 5(c): Branch flow

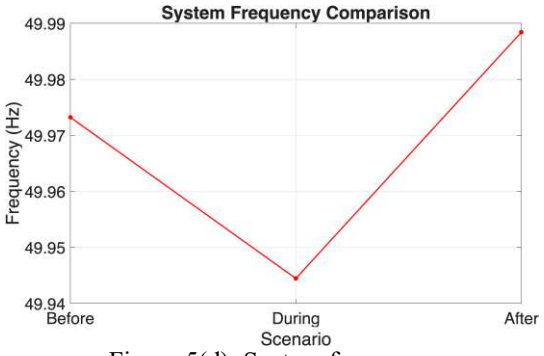


Figure 5(d): System frequency

Figure 5: Case 2: Outage of branches 1-5 and 2-5 (Voltage range: 0.97-1.03 p. u.).

Case 3 (Figure 6) considers outages of branches 12-13 and 13-14 with a voltage range of 0.95-1.05 p. u.. Voltage drops are more localized, primarily affecting buses near the radial ends. Post-redispatch recovery is effective but less uniform than Case 1, reflecting the impact of contingency location. Fewer generators participate, with the optimization prioritizing those electrically closer to the affected area, enhancing control efficiency. Branch loadings increase noticeably during the outage, and while redispatch partially relieves congestion, topology-dependent stress remains in radial sections. Frequency deviations are similar to Case 1 and recover smoothly, indicating that system-wide power balance is maintained despite localized stresses. Case 4 (Figures 7a-d) applies the same outages as Case 3 with tighter voltage limits (0.97–1.03 p.u.). Voltage recovery is more constrained but less uniform than Case 2, revealing structural weaknesses in electrically remote buses and highlighting the diagnostic value of strict voltage constraints. Generator redispatch is more distributed, branch loadings are further reduced, and frequency deviations remain minimal. While tighter limits enhance overall system security, they require greater coordination, which the algorithm effectively achieves.

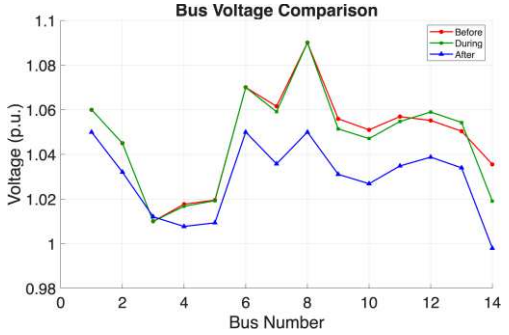


Figure 6(a): Bus voltage

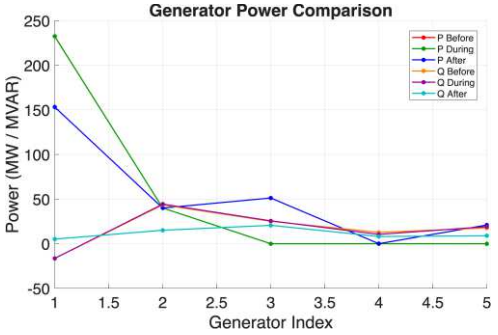


Figure 6(b): Generator power

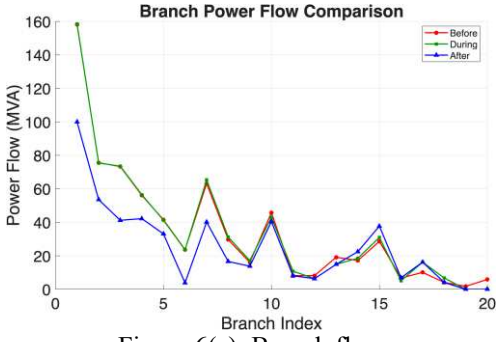


Figure 6(c): Branch flow

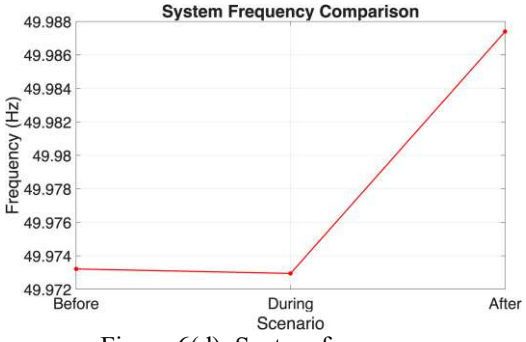


Figure 6(d): System frequency

Figure 6: Case 3: Outage of branches 12-13 and 13-14 (Voltage range: 0.95-1.05 p. u.).

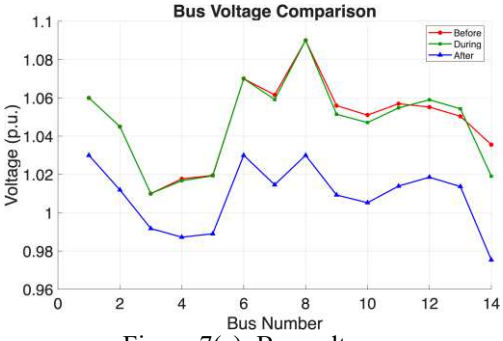


Figure 7(a): Bus voltage

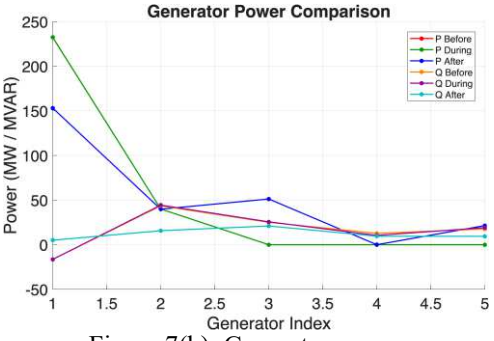


Figure 7(b): Generator power

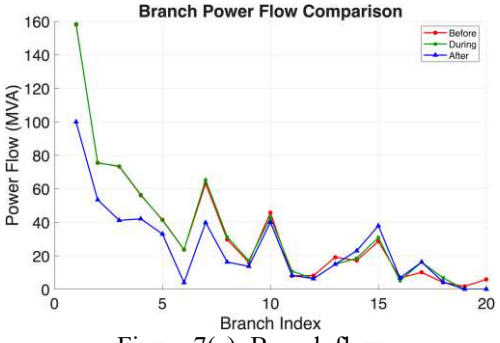


Figure 7(c): Branch flow

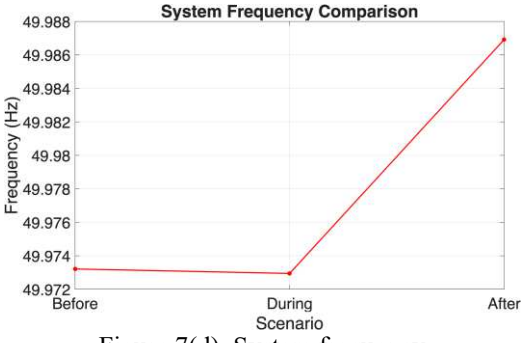


Figure 7(d): System frequency

Figure 7: Case 4: Outage of branches 12-13 and 13-14 (Voltage range: 0.97-1.03 p. u.).

The proposed solution has been successfully to correct the power flow in terms of voltage limits, branch limits and frequency limit during N-2 line outage across all the scenarios when bechmarked test with IEEE 14-bus test system. Different N-2 branches were trippend and voltage striction have applied but the proposed solution performed outstandingly and successful to optimizing the power flow during contingencies in deverse scenario.

3.2 Results for IEEE-118 Bus Test System (Case: 4-8)

To validate scalability, the proposed generator redispatch strategy was tested on the IEEE 118-bus system, representing a realistic large-scale network. Figures 8-11 show that, during contingencies, voltage deviations are smaller than in the 14-bus system, but redispatch involves more generators, reflecting increased coordination requirements. Cases 5 and 6 simulate simultaneous tripping of branches 19-34 and 27-70 under voltage limits of 0.95-1.05 p. u. and 00.97-1.03 p. u., respectively. In both cases, post-redispatch voltages remain within limits, generator adjustments are individually modest but collectively

effective, and branch loadings are redistributed rather than fully eliminated. These results demonstrate that the method scales efficiently through coordinated, distributed corrections, maintaining system security in larger networks. Following the analysis on the IEEE 14-bus system, an N-2 contingency involving simultaneous tripping of branches 5-6 and 12-117 was examined on the IEEE 118-bus system to validate the proposed optimization strategy in a larger network. Cases 7 and 8 correspond to the same line outages under voltage limits of 0.95-1.05p. u. and 0.97-1.03p. u., respectively.

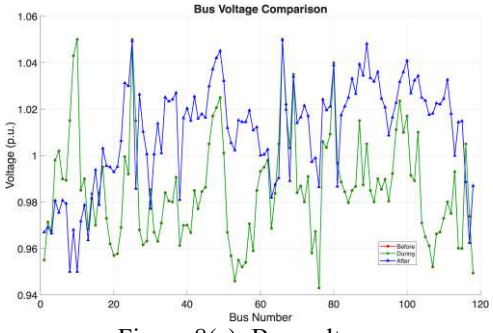


Figure 8(a): Bus voltage

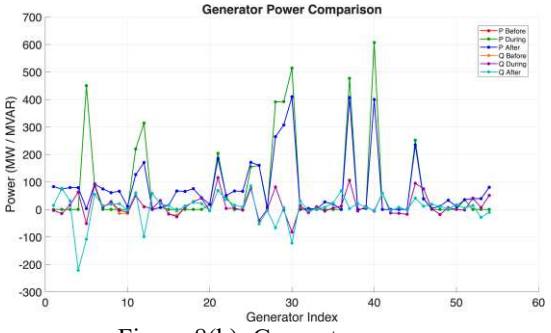


Figure 8(b): Generator power

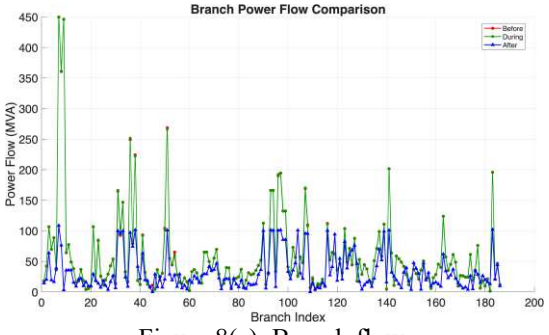


Figure 8(c): Branch flow

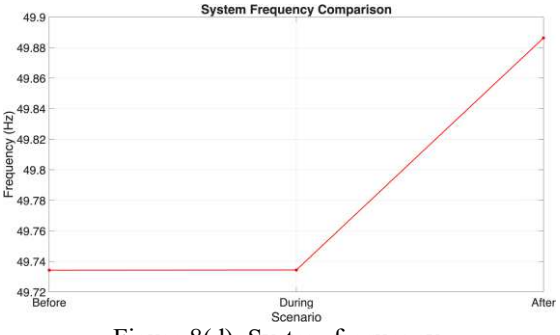


Figure 8(d): System frequency

Figure 8: Case 5: Outage of branches 19-34 and 27-70 (Voltage range: 0.95-1.05 p. u.).

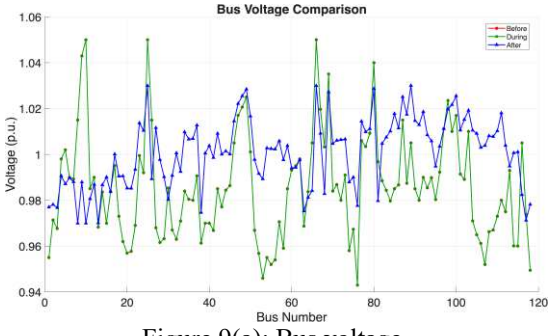


Figure 9(a): Bus voltage

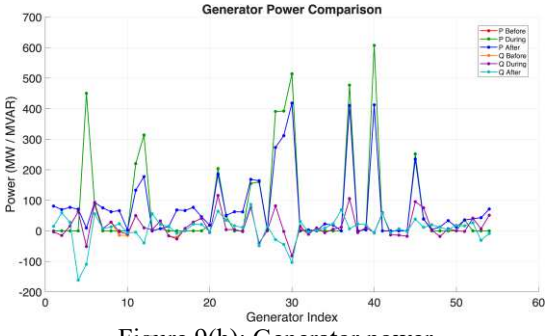


Figure 9(b): Generator power

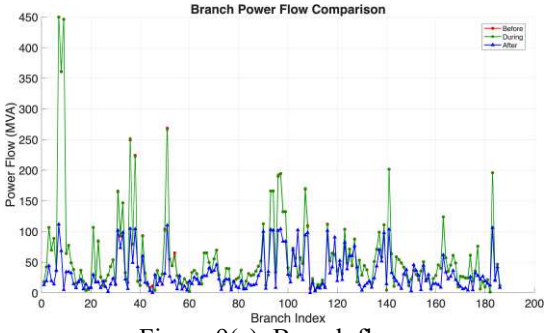


Figure 9(c): Branch flow

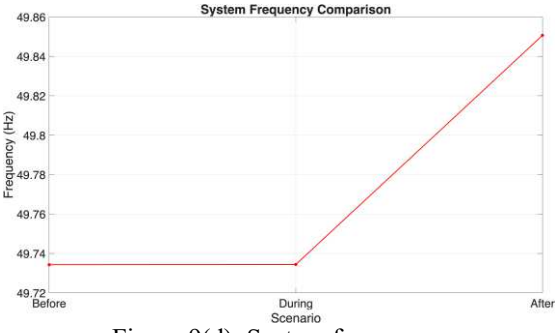


Figure 9(d): System frequency

Figure 9: Case 6: Outage of branches 19-34 and 27-70 (Voltage range: 0.97-1.03 p. u.).

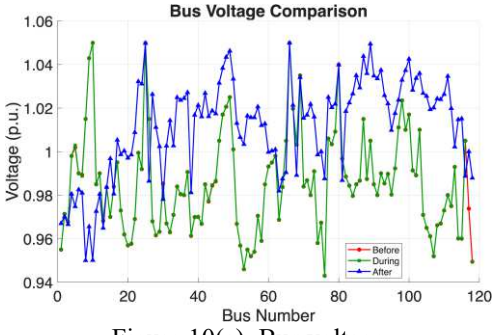


Figure 10(a): Bus voltage

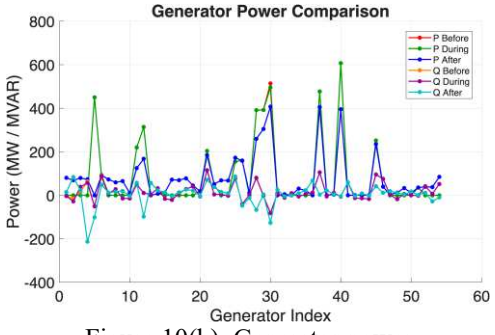


Figure 10(b): Generator power

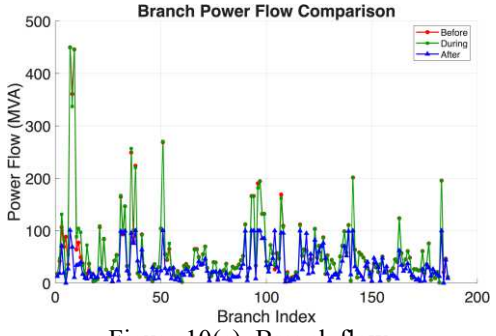


Figure 10(c): Branch flow

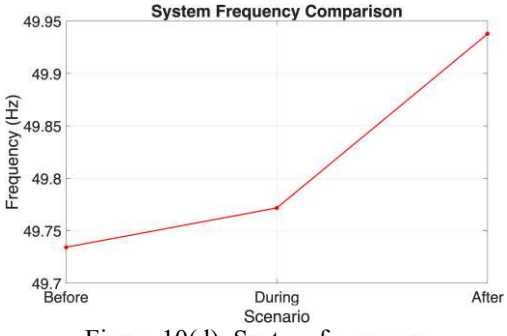


Figure 10(d): System frequency

Figure 10: Case 7: Outage of branches 5-6 and 12-117 (Voltage range: 0.95-1.05 p. u.).

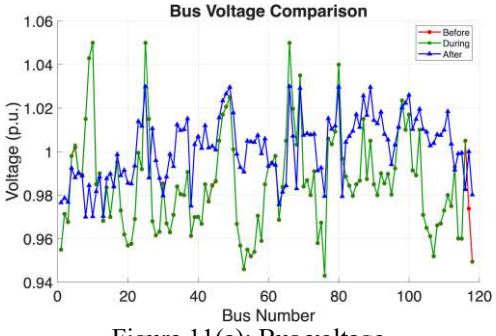


Figure 11(a): Bus voltage

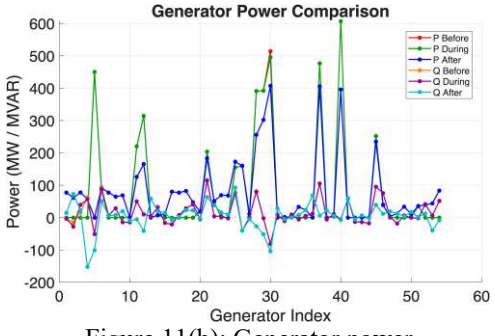


Figure 11(b): Generator power

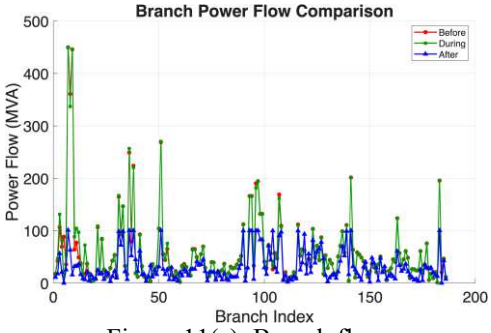


Figure 11(c): Branch flow

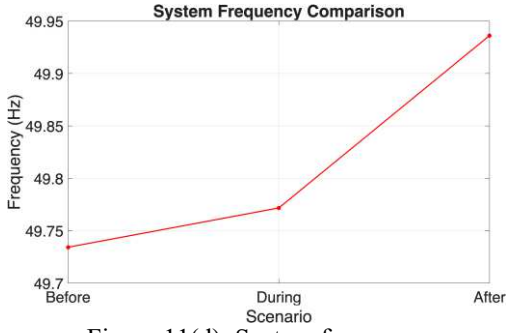


Figure 11(d): System frequency

Figure 11: Case 8: Outage of branches 5-6 and 12-117 (Voltage range: 0.97-1.03 p. u.).

The results show that while outage locations create distinct stress patterns, the generator redispatch effectively restores voltages within limits, demonstrating the approach's adaptability, robust convergence, and consistent solution quality across different operating conditions.

3.3 Metrics Evaluation and Performance Improvement

The effectiveness of the proposed corrective generator redispatch strategy under multiple N-2 line outages was evaluated using quantitative metrics for voltage, branch thermal limits, and system frequency. The bus voltage improvement, I_v (%) is calculated as (23).

$$I_v\,(\%) = \frac{B_a - B_d}{B_t} \times 100 \tag{23}$$

Where B_d and B_a denote the number of buses within voltage limits during the contingency and after OPF redispatch, respectively, and B_t is the total number of buses. The branch thermal compliance improvement, I_b (%) is computed as (24).

$$I_b\,(\%) = \frac{Br_a - Br_d}{Br_t} \times 100 \tag{24}$$

Where Br_d and Br_a represent the number of branches within thermal limits during contingency and after redispatch, respectively, and Br_t is the total number of active branches (excluding tripped lines). System frequency performance is assessed relative to the nominal frequency, $f_{base} = 50\text{Hz}$. The improvement, I_f is defined as (25).

$$I_f\,(\text{Hz}) = |f_d - f_{base}| - |f_a - f_{base}| \tag{25}$$

Where f_d and f_a are the system frequencies during the contingency and after redispatch. Table 3 consolidates all performance metrics for Cases 1-8.

Table 3: System performance improvement during N-2 contingencies after corrective OPF redispatch

Case	B_d	B_a	B_t	I_v(%)	Br_d	Br_a	Br_t	I_b(%)	f_d	f_a	I_f(Hz)
1	8	14	14	42.86	15	18	18	16.67	0.056	0.011	0.045
2	3	14	14	78.57	15	18	18	16.67	0.056	0.012	0.044
3	6	14	14	57.14	17	18	18	5.56	0.027	0.013	0.014
4	4	14	14	71.43	17	18	18	5.56	0.027	0.013	0.014
5	115	118	118	2.54	158	172	184	7.61	0.266	0.114	0.152
6	78	118	118	33.9	158	171	184	7.07	0.266	0.149	0.116
7	114	118	118	3.39	156	173	184	9.24	0.228	0.062	0.166
8	77	118	118	34.75	156	172	184	8.7	0.228	0.064	0.164

Results in Table 3 confirm the effectiveness of the corrective redispatch strategy under N-2 contingencies. Voltage compliance improved significantly, with up to 78.57% of buses restored within limits. Branch flow compliance also increased, with smaller systems showing larger gains due to fewer active branches, while larger systems achieved moderate improvements from distributed adjustments. Frequency deviations were reduced in all cases, by up to 0.166Hz, reflecting improved power balance and system stability. These results demonstrate that the redispatch effectively mitigates voltage, thermal, and frequency violations, with performance influenced by system size, contingency severity, topology, and generator flexibility. Computation time is critical for corrective control, as delays can increase system stress and cascading risk. Figure 12 shows execution times for Cases 1-8 using MATLAB's tic – toc. For the IEEE 14-bus system (Cases 1-4), times are stable at 2.8-3.1s, showing minimal impact from outage location or voltage limits. For the IEEE 118-bus system (Cases 5-6), computation exceeds 4s, with Case 6 highest due to more buses, generators, and control variables. Cases 7-8 show reduced times despite the same system size, reflecting the influence of outage location and network stress on convergence. Overall, execution scales with system size, stays below 4.5s, and depends on topology, confirming suitability for real-time or near-real-time implementation.



Figure 12: Execution time comparison.

4. Conclusion and Future Works

This paper presents a multi-phase corrective redispatch framework for restoring voltage, frequency, and line limits under N-2 contingencies. By systematically redistributing active and reactive power while enforcing voltage, generator, and branch constraints, the framework ensures post-contingency system security. Simulations on the IEEE 14-bus and 118-bus systems demonstrate full voltage compliance, with maximum improvements of 78.57% for bus voltages, 16.67% for branch overload relief, and 0.166Hz for frequency deviation, while maintaining computation times under 4.5 s. Future work will extend the framework to incorporate inverter-based resources, dynamic frequency assessment, expanded corrective actions (load shedding, demand response, network reconfiguration), uncertainty-aware optimization, and large-scale EMS integration. Overall, the study delivers a scalable, efficient, and practical tool for real-time post-contingency control, bridging the gap between traditional steady-state screening and actionable operational decision-making.

Funding
Not available.

Data Availability
All the relevant data have been included in this paper. Additional data can be provided upon request.

Declaration of Competing Interest
The authors affirm that no known completing financial interests or personal relationships could have influenced the work reported in this paper.

Acknowledgement
This research work was supported by the Ministry of Higher Education (MoHE), the Faculty of Engineering and Technology, i-CATS University College and Universal University of Science, Engineering & Technology. All authors have read and agreed to publish the version of the manuscript.

References

[1] N. Bhusal, M. Abdelmalak, M. Kamruzzaman, and M. Benidris, "Power System Resilience: Current Practices, Challenges, and Future Directions," IEEE Access, vol. 8, pp. 18064–18086, 2020, doi: 10.1109/ACCESS.2020.2968586.
[2] Z. M. Ali, M. Ćalasan, F. Jurado, and S. H. E. Abdel Aleem, "Complexities of Power Quality and Harmonic-Induced Overheating in Modern Power Grids Studies: Challenges and Solutions," IEEE Access, vol. 12, pp. 151554–151597, 2024, doi: 10.1109/ACCESS.2024.3477729.
[3] S. A. Adegoke and Y. Sun, "Power system optimization approach to mitigate voltage instability issues: A review," Cogent Eng., vol. 10, no. 1, Dec. 2023, doi: 10.1080/23311916.2022.2153416.
[4] V. Veerasamy et al., "Recurrent network based power flow solution for voltage stability assessment and improvement with distributed energy sources," Appl. Energy, vol. 302, p. 117524, Nov. 2021, doi: 10.1016/j.apenergy.2021.117524.
[5] Y. Gui et al., "Review of Challenges and Research Opportunities for Control of Transmission Grids," IEEE Access, vol. 12, pp. 94543–94569, 2024, doi: 10.1109/ACCESS.2024.3425272.
[6] M. Boruni, M. Torabi, M. A. Latify, G. R. Yousefi, and J. Aghaei, "Critical contingencies-aware conic AC transmission network expansion and reactive power co-planning," Sustainable Energy, Grids and Networks, vol. 44, p. 101960, Dec. 2025, doi: 10.1016/j.segan.2025.101960.
[7] P. A. Moulum, J. J. Mandeng, and C. H. Kom, "Holistic analysis of the dynamic stability of the Southern Cameroon Interconnected grid in contingency situations," Sci. Afr., vol. 26, p. e02446, Dec. 2024, doi: 10.1016/j.sciaf.2024.e02446.
[8] A. Amarendra, L. R. Srinivas, and R. S. Rao, "Contingency Analysis in Power System- Using UPFC and DVR Devices with RDOA," Technology and Economics of Smart Grids and Sustainable Energy, vol. 7, no. 1, p. 17, Apr. 2022, doi: 10.1007/s40866-022-00129-y.
[9] L. S. Mahendra, R. Delfianti, K. Nisa, B. Mustaqim, C. Harsito, and R. C. Syahroni, "Security-Constrained Optimal Power Flow in Renewable Energy-Based Microgrids Using Line Outage Distribution Factor for Contingency Management," Energy Engineering, vol. 122, no. 7, pp. 2695–2717, 2025, doi: 10.32604/ee.2025.063807.
[10] N. Misra, K. T. Chaturvedi, and A. K. Sharma, "A Real Time Approach to Determine ATC and TTC for a Secure Interconnected Power Transmission System," Journal of The Institution of Engineers (India): Series B, Sep. 2025, doi: 10.1007/s40031-025-01266-5.
[11] I. Asensio Bermejo, H. Foretić, V. Kopustinskas, and G. Fulli, "Resilience assessment of a power system due to disruption of interconnectors," Environ. Syst. Decis., vol. 45, no. 3, p. 48, Sep. 2025, doi: 10.1007/s10669-025-10041-2.
[12] S. Nandini P and R. Krishan, "Enhanced voltage stability assessment and remedial action schemes for resilient power systems under cascading contingencies," Reliab. Eng. Syst. Saf., vol. 270, p. 112154, Jun. 2026, doi: 10.1016/j.ress.2025.112154.
[13] B. Wang et al., "A four-stage fast reliability assessment framework for renewables-dominated strong power systems with large-scale energy storage by temporal decoupling and contingencies filtering," Appl. Energy, vol. 362, p. 123035, May 2024, doi: 10.1016/j.apenergy.2024.123035.
[14] H. Mubarak et al., "Optimum Distribution System Expansion Planning Incorporating DG Based on N-1 Criterion for Sustainable System," Sustainability, vol. 13, no. 12, p. 6708, Jun. 2021, doi: 10.3390/su13126708.
[15] A. Stankovski, B. Gjorgiev, L. Locher, and G. Sansavini, "Power blackouts in Europe: Analyses, key insights, and recommendations from empirical evidence," Joule, vol. 7, no. 11, pp. 2468–2484, Nov. 2023, doi: 10.1016/j.joule.2023.09.005.
[16] G. Fotis, V. Vita, and T. I. Maris, "Risks in the European Transmission System and a Novel Restoration Strategy for a Power System after a Major Blackout," Applied Sciences, vol. 13, no. 1, p. 83, Dec. 2022, doi: 10.3390/app13010083.
[17] B. A. Carreras, D. E. Newman, and I. Dobson, "North American Blackout Time Series Statistics and Implications for Blackout Risk," IEEE Transactions on Power Systems, vol. 31, no. 6, pp. 4406–4414, Nov. 2016, doi: 10.1109/TPWRS.2015.2510627.
[18] C. Lehmkoster, "Security constrained optimal power flow for an economical operation of FACTS-devices in liberalized energy markets," IEEE Transactions on Power Delivery, vol. 17, no. 2, pp. 603–608, Apr. 2002, doi: 10.1109/61.997946.
[19] E. Karangelos and L. Wehenkel, "An Iterative AC-SCOPF Approach Managing the Contingency and Corrective Control Failure Uncertainties With a Probabilistic Guarantee," IEEE Transactions on Power Systems, vol. 34, no. 5, pp. 3780–3790, Sep. 2019, doi: 10.1109/TPWRS.2019.2902486.
[20] A. Agarwal, P. L. Donti, J. Z. Kolter, and L. Pileggi, "Large Scale Bilevel Optimization for N-K SCOPF Using Adversarial Robustness," IEEE Transactions on Power Systems, vol. 40, no. 6, pp. 5209–5220, Nov. 2025, doi: 10.1109/TPWRS.2025.3579521.
[21] P. Sidor and S. Robak, "Transmission-Targeted Demand-Side Response for Congestion Relief: A Systematic Review," Energies (Basel)., vol. 18, no. 21, p. 5705, Oct. 2025, doi: 10.3390/en18215705.
[22] A. Bhiryani, P. Haritz, and T. Liebig, "Jacobian-Based Adversarial Attacks for N-1 Robust Power Grid Control," in 2025 IEEE Kiel PowerTech, IEEE, Jun. 2025, pp. 1–6. doi: 10.1109/PowerTech59965.2025.11180724.
[23] M. Liu, M. Liao, R. Zhang, X. Yuan, Z. Zhu, and Z. Wu, "Quantum Computing as a Catalyst for Microgrid Management: Enhancing Decentralized Energy Systems Through Innovative Computational Techniques," Sustainability, vol. 17, no. 8, p. 3662, Apr. 2025, doi: 10.3390/su17083662.
[24] G. M. Njoka, L. Mogaka, and A. Wangai, "Enhancing grid stability and resilience through BESS optimal placement and sizing in VRES-dominated systems," Energy Reports, vol. 13, pp. 1764–1779, Jun. 2025, doi: 10.1016/j.egyr.2025.01.028.
[25] L. Sun, W. Fang, Y. Wei, Z. Lin, and X. Jin, "Robust contingency-constrained load restoration method for transmission systems considering modified SOCP formulation of power flow," International Journal of Electrical Power & Energy Systems,

vol. 163, p. 110345, Dec. 2024, doi: 10.1016/j.ijepes.2024.110345.
[26] M. Heidarifar, P. Andrianesis, P. Ruiz, M. C. Caramanis, and I. Ch. Paschalidis, “An optimal transmission line switching and bus splitting heuristic incorporating AC and N-1 contingency constraints,” International Journal of Electrical Power & Energy Systems, vol. 133, p. 107278, Dec. 2021, doi: 10.1016/j.ijepes.2021.107278.
[27] P. A. Moulum, J. J. Mandeng, and C. H. Kom, “Optimal SVC allocation for enhancing modern power network stability using a max–min aggregation based multi-criteria hybrid CF-PSO FAHP algorithm considering N-1 contingencies,” International Journal of Electrical Power & Energy Systems, vol. 172, p. 111192, Nov. 2025, doi: 10.1016/j.ijepes.2025.111192.
[28] S. I. Ocean, K. Cantley, and E. Hossain, “Quantifying power system strength to identify unique credible contingencies in renewable-dominated power systems,” International Journal of Electrical Power & Energy Systems, vol. 172, p. 111271, Nov. 2025, doi: 10.1016/j.ijepes.2025.111271.
[29] A. Kumar and T. Ghose, “An AC Z-bus-based distribution factors for contingency analysis of AC–DC networks,” Electric Power Systems Research, vol. 238, p. 111104, Jan. 2025, doi: 10.1016/j.epsr.2024.111104.
[30] M. Manojkumar, V. Sundaravazhuthi, B. Ponmudi, T. D. Raj, and S. Swaminathan, “Performance analysis of credible contingency selection schemes for security enhancement in power system network,” Electric Power Systems Research, vol. 246, p. 111653, Sep. 2025, doi: 10.1016/j.epsr.2025.111653.
[31] X. Zheng, A. Lee, S. Hsien Huang, and L. Xie, “A Physics-Informed Graph Neural Network Framework for N-2 Contingency Screening: A Real-World Texas Grid Study,” IEEE Open Access Journal of Power and Energy, vol. 12, pp. 784–792, 2025, doi: 10.1109/OAJPE.2025.3626699.
[32] C. D. Iweh, S. Gyamfi, E. Effah-Donyina, and E. Tanyi, “Analysis of contingency scenarios towards a suitable transmission pathway in the southern interconnected grid (SIG) of Cameroon,” e-Prime - Advances in Electrical Engineering, Electronics and Energy, vol. 7, p. 100486, Mar. 2024, doi: 10.1016/j.prime.2024.100486.
[33] Y. Zhao, W. Gan, M. Yan, J. Wen, and Y. Zhou, “A scalable stochastic scheme for identifying critical substations considering the epistemic uncertainty of contingency in power systems,” Appl. Energy, vol. 381, p. 125119, Mar. 2025, doi: 10.1016/j.apenergy.2024.125119.
[34] A. Sengupta and S. Das, “Transient stability-constrained optimal rescheduling of generation for post-contingency secure operation of power systems during load encroachment,” Electrical Engineering, vol. 107, no. 8, pp. 10805–10824, Aug. 2025, doi: 10.1007/s00202-025-03062-2.
[35] M. Thulasingam and A. D. V. R. Periyanayagam, “Radial distribution systems performance enhancement through RE (Renewable Energy) integration and comprehensive contingency ranking analysis,” Green Energy and Intelligent Transportation, vol. 4, no. 1, p. 100245, Feb. 2025, doi: 10.1016/j.geits.2024.100245.
[36] H. Shi, S. Cai, Y. Xie, Q. Wu, and J. Sun, “A robust microgrid formation method for risk-resistant service restoration considering subsequent contingency,” International Journal of Electrical Power & Energy Systems, vol. 159, p. 109994, Aug. 2024, doi: 10.1016/j.ijepes.2024.109994.
[37] F. Feng, Y. Zhou, M. A. Bragin, Y. A. Shamash, and P. Zhang, “Quantum contingency analysis for power system steady-state security identification,” Sci. Rep., vol. 15, no. 1, p. 15148, Apr. 2025, doi: 10.1038/s41598-025-98776-5.
[38] D. K. Dhaked, D. K. Goyal, V. L. Narayanan, Y. Gopal, and D. Birla, “Ensemble Learning Based Method for Contingency Classification and Ranking in a Large Power System,” Next Research, vol. 2, no. 4, p. 100964, Dec. 2025, doi: 10.1016/j.nexres.2025.100964.
[39] S. Mokred, Y. Wang, and T. Chen, “A Novel Collapse Prediction Index for Voltage Stability Analysis and Contingency Ranking in Power Systems,” Protection and Control of Modern Power Systems, vol. 8, no. 1, pp. 1–27, Jan. 2023, doi: 10.1186/s41601-023-00279-w.
[40] N. M. Ndjankeu, P. A. Moulum, P. Kenfack, and S. R. D. Naoussi, “Modern sensitivity index-based optimal UPFC location for power quality enhancement in the Southern Cameroon interconnected grid considering the feasibility of the load flow under N-k contingency scenarios,” Energy Reports, vol. 13, pp. 5160–5186, Jun. 2025, doi: 10.1016/j.egyr.2025.04.049.
[41] S. Song, S. Min, and S. Jung, “Steady-state data-driven dynamic stability assessment in the Korean power system,” Sci. Rep., vol. 15, no. 1, p. 7756, Mar. 2025, doi: 10.1038/s41598-025-90798-3.
[42] T. Kërçi and F. Milano, “A Comprehensive Approach to Evaluate Frequency Control Strength of Power Systems,” IEEE Open Access Journal of Power and Energy, vol. 13, pp. 39–50, 2026, doi: 10.1109/OAJPE.2025.3643748.
[43] N. S. Darwade and S. T. Nagarajan, “Voltage Angle Based Power System Inertia Estimation Using Synchrophasor Technology,” Journal of Electrical Engineering & Technology, vol. 20, no. 6, pp. 3925–3941, Sep. 2025, doi: 10.1007/s42835-025-02305-3.
[44] S. Yuan, L. Y. Wang, G. Yin, and M. H. Nazari, “Contingency detection in modern power systems: A stochastic hybrid system method,” Sustainable Energy, Grids and Networks, vol. 39, p. 101414, Sep. 2024, doi: 10.1016/j.segan.2024.101414.
[45] A. S. Altgott and I. D. Melo, “Power system contingency assessment considering harmonic distortions: a sensitivity analysis based on the compensation theorem,” Electrical Engineering, vol. 106, no. 4, pp. 5043–5054, Aug. 2024, doi: 10.1007/s00202-024-02299-7.
[46] S. Li, J. Shao, S. Zhang, and H. Chen, “Distribution network reconfiguration incorporating thermostatic loads after multiple line contingency,” Energy Reports, vol. 13, pp. 813–823, Jun. 2025, doi: 10.1016/j.egyr.2024.12.061.
[47] F. Bereta Dos Reis et al., “Modeling Puerto Rico Grid’s Sequential Failures for Hurricanes Using Electric Grid Resilience & Assessment System (EGRASS) Tool and Dynamic Contingency Analysis Tool (DCAT),” IEEE Access, vol. 13, pp. 67446–67458, 2025, doi: 10.1109/ACCESS.2025.3555144.
[48] R. Ithaya, N. Kanthavelkumaran, N. Visalatchi, and A. Saravanan, “Reliability Analysis of Power System Using a Multinomail Monte Carlo Simulation,” Technical Physics Letters, vol. 51, no. 8, pp. 320–333, Aug. 2025, doi: 10.1134/S1063785025600565.
[49] O. Sadeghian, B. Mohammadi-Ivatloo, M. Abapour, and J. Aghaei, “Proactive Resilience-Focused Operation of Power System Against Random and Intelligent Attacks,” IEEE Access, vol. 14, pp. 19224–19248, 2026, doi: 10.1109/ACCESS.2026.3658934.

[50] K. Jiang, S. Lin, Y. Yang, L. Deng, and M. Liu, “Optimal preventive control for static voltage stability of integrated transmission and distribution networks under multiple N-1 contingencies considering uncertain renewables,” International Journal of Electrical Power & Energy Systems, vol. 175, p. 111617, Feb. 2026, doi: 10.1016/j.ijepes.2026.111617.
[51] W. Tian, S. Cai, Y. Xie, C. Yu, H. Wu, and Q. Wu, “A risk-resistant microgrid formation method considering subsequent line faults and outage propagation,” International Journal of Electrical Power & Energy Systems, vol. 173, p. 111399, Dec. 2025, doi: 10.1016/j.ijepes.2025.111399.